Reflection Analysis of PML ABC's for Low-Frequency Applications

Jan De Moerloose, *Member, IEEE,* and Maria A. Stuchly, *Fellow, IEEE*

***Abstract*—A basic numerical reflection analysis is presented for low-frequency applications using a new type of the reflectivity diagram. The retardation effect at low frequencies is explained and use of an exponential profile, as suggested.**

I. Introduction

BERENGER'S perfectly matched layer (PML) technique [1] is superior to most standard absorbing boundary conditions (ABC's) by orders of magnitude [1], [2]. Its performance has been adequately explained from an analytical standpoint [1], [3], but a more detailed analysis is necessary of a numerical grid reflection. A substantial numerical reflection occurs in the evanescent wave region, esspecially in the low-frequency region [4]. In this letter, we show that this numerical reflection strongly depends on the conductivity profile. High reflectivity levels in the low-frequency region are mentioned in [4] as a probable cause of problems for low-frequency simulations. Here, we show that the propagation speed within the PML gets progressively lower with decreasing frequency, which leads to a retardation effect. For an exponential profile, the retardation time is inversely proportional to frequency. This property makes this profile extremely useful for low-frequency applications.

II. Comparison of PML Profiles by the Reflectivity Diagram

The plane wave reflectivity $\mathbf{r}_p$ of an absorbing boundary can generally be obtained by dividing the complex amplitude of the reflected field $\mathbf{R}$ by the complex amplitude of the incident field $\mathbf{I}$

$$\mathbf{r}_p(\omega, k_y) = |\mathbf{r}_p| \exp(j\varphi) = \frac{\mathbf{R}(\omega, k_y)}{\mathbf{I}(\omega \cdot k_y)}. \quad (1)$$

For two-dimensional problems and an absorbing boundary parallel to the y-axis, $\mathbf{r}_p$ depends on the radial frequency ω and the transverse wavenumber k_y, whose value is a function of the angle of incidence. For an infinite plane and most absorbing boundary conditions, $\mathbf{r}_p$ can be calculated analytically. For PML, a multiple transmission line technique is recommended (see e.g., [4] and [5]). Since $\mathbf{r}_p$ depends on both ω and k_y, a complete picture of the reflective behavior is given by a color-coded graph of $|\mathbf{r}_p|$ with ω on the x axis and k_y on the y axis. In this representation, all points below the diagonal $(\omega/c > k_y)$ correspond to propagating waves and all points above the diagonal $(\omega/c < k_y)$ correspond to evanescent waves. The diagonal $(\omega/c = k_y)$ represents waves at the grazing incidence or cutoff. All points that correspond to a propagating wave at a fixed angle of incidence are situated on a straight line intersecting the origin.

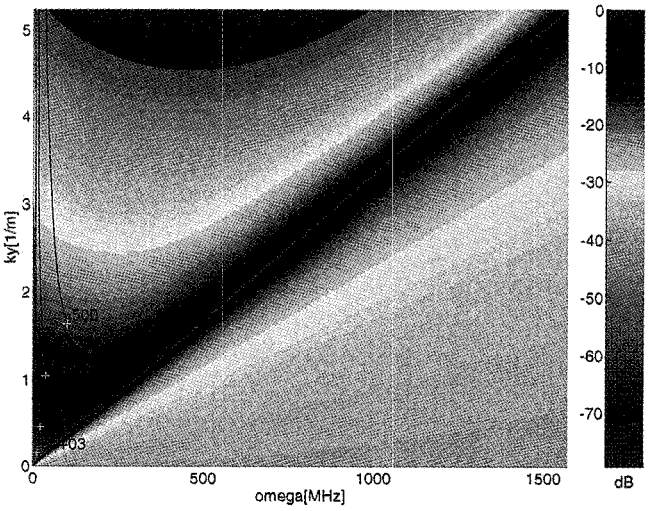

Fig. 1. Reflectivity diagram for a PML(4, P, 1) (color → $|\mathbf{r}_p|$, contours → t_0).

Figs. 1 and 2 show the reflectivity diagram of a PML(15, P, 1) and a PML(4, P, 1), respectively. Note that the first number in the brackets after PML denotes the number of layers, the second symbol the conductivity profile (P = parabolic), and the third the reflection coefficient at normal incidence in percent. The reflectivity coefficients are computed at a distance of 15 cells ($\delta = \delta x = \delta y = 0.06$ m) from the outer boundary (an electric wall) in both cases. This means that the natural damping of the evanescent waves is the same in both cases, i.e., we prefer to look at the PML(4, P, 1) as a 15-cell layer with a different conductivity profile than the PML(15, P, 1). For a continuous space, the reflection coefficient of a PML layer is determined by its width for evanescent waves and by the normal reflection coefficient for propagating waves [1], [4]. Therefore, from a purely analytical viewpoint, both PML layers should behave identically. This is to a large degree correct in the propagating region but not in the evanescent region (see Figs. 1 and 2). Although the behavior around the cutoff region is very similar, the low-frequency and the intermediate regions are clearly

Manuscript received November 11, 1995. This work was supported by the Natural Sciences and Engineering Research Council of Canada (NSERC), BC Hydro, and TransAlta Utilities.

The authors are with the Department of Electrical and Computer Engineering, University of Victoria, Victoria, British Columbia V8W 3P6, Canada.

Publisher Item Identifier S 1051-8207(96)02580-9.

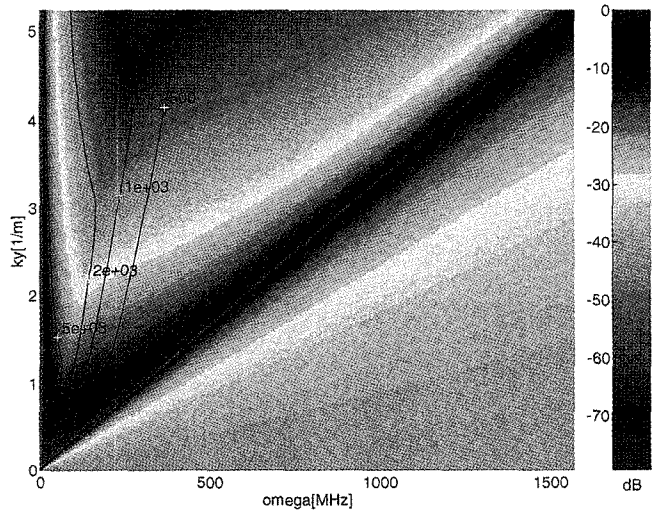

Fig. 2. Reflectivity diagram for a PML(15, P, 1) (color $\rightarrow |\mathbf{r}_p|$, contours $\rightarrow t_0$).

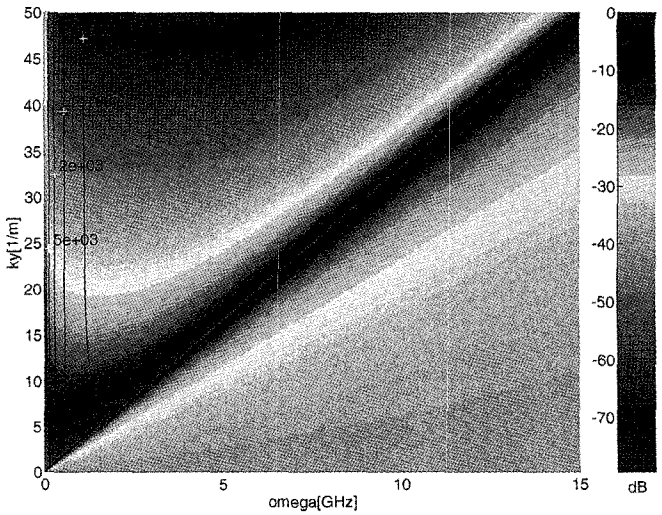

Fig. 3. Reflectivity diagram for a PML(15, exponential; $A = 0.9102, 1$) (color $\rightarrow |\mathbf{r}_p|$, contours $\rightarrow t_0$).

different for the two cases. While there is a slightly stronger absorption for the intermediate region for the PML(15, P, 1), the opposite is true for very low frequencies. In fact, the reflectivity tends to one in the static case for all transverse wavelengths, in accordance with [4]. This behavior is rather worrying, as it could possibly inhibit the use of PML in low-frequency modeling.

III. Retarded Reflections and the Exponential Profile

A general component of an evanescent plane wave in a PML medium contains a phase factor $\exp(j\frac{\sigma_x k_x x}{\varepsilon_0 \omega})$ [4]. (k_x is the imaginary part of the commonly used wavenumber.) The PML medium can therefore be looked upon as a dispersive medium with a characteristic group velocity v_g, given by

$$\frac{1}{v_g} = -\frac{\partial}{\partial \omega}\left(\frac{\sigma_x k_x}{\varepsilon_0 \omega}\right)_{ky=\text{cst}} = \frac{\sigma_x k_y^2}{\varepsilon_0 \omega^2 k_x}. \tag{2}$$

Very low group velocities may occur at low frequencies ($\omega \approx 0$) and near the cutoff region ($k_x \approx 0$). This means that reflected waves propagate slowly through the PML medium and appear only after a certain delay, here called the retardation time. Using (2) to calculate the retardation time is rather complicated, since the reflections do not always occur at the end of the layer and (2) is strictly speaking valid for a continuous medium only. A more practical way to calculate the retardation time t_0 is from the phase of the reflection coefficient (1)

$$t_0 = -\left(\frac{\partial \varphi}{\partial \omega}\right)_{k_y=\text{cst}}. \tag{3}$$

Numerically computed retardation times are superimposed in Figs. 1 and 2, as a contour plot. The contours are labeled by the number of timesteps $\delta t = \delta/(2c)$. The retardation times are much larger for the PML(15, P, 1) and effectively window out high amplitude reflections in the low-frequency region. Results in Figs. 1 and 2 are analytical, but they take into account the numerical dispersion of the grid. The entirely numerical calculations performed but not cited here indeed confirm that the reflections increase with increasing simulation time. We also notice that for a parabolic profile, the retardation time is dependent on frequency as well as transverse wavelength. This makes it very difficult to determine the retardation time for an actual problem since usually there is no information available on the transverse wavelength.

For the exponential profile, retardation times will be shown to depend on frequency only. Starting with the fact that numerical reflections at low frequency occur [4] when

$$\frac{\sigma_x k_x \delta}{\varepsilon_0 \omega} \approx \pi \tag{4}$$

and assuming σ_x to be monotonically increasing and condition (4) to be fulfilled after the wave has traveled over a distance x, the retardation time is given by

$$t_0 = 2\int_0^x \frac{dx'}{v_g} \approx 2\int_0^x \frac{\sigma_x(x') k_x}{\varepsilon_0 \omega^2} dx'. \tag{5}$$

To obtain the last approximation in (5), (2) and $k_x \approx k_y$ were used for low frequencies. This expression is dependent only on ω, after k_x is eliminated by substituting (4)

$$t_0 \approx \frac{2\pi}{\omega \delta}\frac{1}{\sigma_x}\int_0^x \sigma_x(x')dx'. \tag{6}$$

The above expression is still a function of $\sigma_x(x)$ unless $\frac{1}{\sigma_x}\int_0^x \sigma_x(x')dx'$ is a constant A for all x. This condition is best fulfilled (although not exactly because of the lower limit of the integral) by an exponential profile

$$\sigma_x = Be^{x/A}. \tag{7}$$

Our theory is illustrated in Fig. 3 showing the reflectivity diagram for a 15-cell exponential profile with $\delta = 1$ mm and $A = 1/\ln(3) = 0.9102$. The retardation time is obviously to a large degree independent of the transverse wavelength, as predicted. As shown on the logarithmic plot in Fig. 4, its value is very close to $t_0 = \frac{2\pi A}{\omega \delta}$, given by (6). This proves

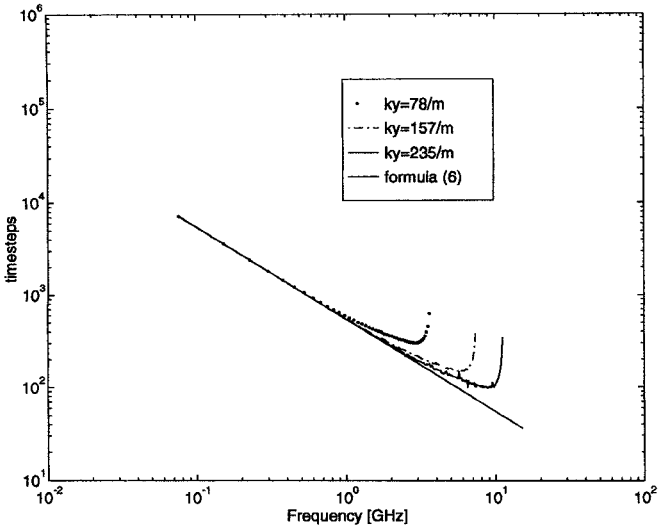

Fig. 4. Retardation time versus frequency for exponential profile.

that our explanation of the basic reflection mechanism at low frequencies is correct. The choice of A is somewhat arbitrary. The magnitude of the reflection coefficient depends on B, but to a lesser extent for evanescent waves than for propagating waves. It is also not of importance as long as the reflections are filtered out by sufficiently short simulation tissues. The retardation mechanism is a time-domain phenomenon, which explains why PML is less effective in frequency-domain methods such as FEM (finite-element modeling).

IV. Conclusion

We have presented a new type of reflectivity diagram to effectively compare PML ABC's (and other ABC's) over the complete frequency range. It was shown that in practical simulations using FDTD (finite-difference time-domain), the high reflections for low frequencies in the evanescent wave region are masked by a retardation mechanism. As a special case, it was shown that for an exponential profile, retardation times are dependent only on frequency.

References

[1] J. P. Berenger, "A perfectly matched layer for the absorption of electromagnetic waves," *J. Comp. Phys.*, vol. 114, pp. 185–200, 1994.

[2] D. S. Katz, E. T. Thiele, and A. Taflove, "Validation and extension to three dimensions of the Berenger PML absorbing boundary condition for FD-TD meshes," *IEEE Microwave Guided Wave Lett.*, vol. 4, pp. 268–271, 1994.

[3] Z. Wu and J. Fang, "Performance of the perfectly matched layer in modeling wave propagation in microwave and digital circuit interconnects," in *Proc. Conf. ACES*, Monterey, CA, Mar. 1995, pp. 504–511.

[4] J. De Moerloose and M. A. Stuchly, "Behavior of Berenger's ABC for evanescent waves," *Microwave Guided Wave Lett.*, vol. 5, pp. 344–346, 1995.

[5] J. De Moerloose and M. A. Stuchly, "An efficient way to compare ABC's," to appear in *IEEE Antennas Propagat. Mag.*